



Sedimental Pollen Distribution in the Northeastern Indian Ocean and their Palaeo-Environmental Information

Chixin Chen¹, Chuanxiu Luo^{2*}, Rong Xiang², Jianguo Liu², Jun Lu², Xiang Su², Qiang Zhang², Sazal Kumar^{2,3}, Lin Yang^{4*}

¹Guangzhou Marine Geological Survey Bureau, Guangzhou

²CAS Key Laboratory of Marginal Sea Geology, South China Sea Institute of Oceanology, Chinese Academy of Sciences, Guangzhou, China

³University of Chinese Academy of Sciences, Beijing, China

⁴Shenzhen Foreign Languages School, Shenzhen, Guangdong, China

***Corresponding Authors:** Chuanxiu Luo, CAS Key Laboratory of Marginal Sea Geology, South China Sea Institute of Oceanology, Chinese Academy of Sciences, Guangzhou, China
Lin Yang, Shenzhen Foreign Languages School, Shenzhen, Guangdong, China

Abstract: Seabed sediments in the northeastern part of the Indian Ocean have preserved comprehensive information of the typical tropical oceans and ancient marine environment. Firstly, the sample of core 12I712 was used for paleoclimate reconstruction of the northeastern Indian Ocean. In zones A and B (45~36 ka BP) of the 12I712 core, tree pollen had a higher percentage. Combined with the high pollen concentration in A and B zones, this reflects the warm and humid climate of the resource areas, which was associated with a high sea level. The percentage of pollen of the trees in zones C and D (36 ~ 5 ka BP) decreased and the percentage of pollen of the herbaceous plants increased. The percentages of pollen from *Betula* and *Alnus* increased, reflecting the gradual transformation to a cold and dry climate with scarce vegetation and drought. Then, based on a fossil pollen analysis on two cores from the northeastern Indian Ocean and compared with fossil pollen results from the South China Sea, we determined that warm pools can be taken as a climate humidity index both in the South China Sea and the Indian Ocean. *Pinus* pollen can be taken as an index of sea level change; its percentage decreased in the low sea level period only in the cores near the continental shelf, and its percentage increased in the low sea level period in the cores in the northeastern Indian Ocean because they are in the deep sea.

Keywords: Pollen; northeastern Indian Ocean; South China Sea; warm pools; climate humidity; sea level change

1. INTRODUCTION

Seabed sediments in the northeastern part of the Indian Ocean have preserved comprehensive information of the typical tropical oceans and ancient marine environment chronicling South Asian monsoon evolution. This area provides a uniquely important opportunity for the high-resolution study of global climate change. Pollen is from terrestrial vegetation the occurrence of pollen in marine sediments reflects the vegetation ecology and climatic conditions on the adjacent terrain. Therefore, conducting research on sedimental pollen in the northeastern Indian Ocean and applying it in Quaternary environmental reconstruction work serves two purposes; to reconstruct ancient terrestrial vegetation succession in the surrounding area, and to track the evolution of ancient historical processes of the marine environment.

The distribution and dissemination of pollen in the northeastern Indian Ocean is closely related to its environmental conditions of hydrothermal power. The terrestrial pollen feature of South and Southeast Asia were studied previously (Leipe et al., 2014a, b; Liang et al., 2015; Riedel et al., 2015; Chauhan et al., 2015; Rawat et al., 2015; Demske et al., 2009; Premathilake and Seneviratne, 2015). The northeastern Indian Ocean is the area of strongest material exchange and most active deposition in the world today, providing experimental conditions of rare tropical deep-sea area edge for the study of ancient climate change.

From the beginning of the 1990s, some studies have discussed the evolutionary role of the Indian monsoon and paleoclimate using foraminiferans and other indicators in the Indian Ocean (Murgese and Deckker, 2005). John et al. (1992) discussed the composition of the foraminifera fauna group in marine sediments controlled by the southwest monsoon in the northwest Arabian Sea using wind, hydro, and marine remote sensing data. Clemens et al. (1991, 1996) reconstructed the strength variance of the Indian summer monsoon in evolutionary history from 530 million years ago, using the abundance of the foraminifera, *Globigerina bulloides* as an indicator of upwelling in the Arabian Sea, combined with deep-sea oxygen isotopes. Prell, (1984a, b) studied Indian summer monsoon change on the scale of the orbit in the northern Arabian Sea, using *G. bulloides* as an indicator of upwelling for time series analysis.

In addition to the studies on foraminifera, research of radiolarians (Gupta, 2003) and Dinoflagellate in the northeastern Indian Ocean has been conducted (Marret and Vernal, 1997); however, few studies have focused on pollen present in drilling cores (Sander and Patrick, 2003). The longest pollen record spans the last 200 thousand years in the neighboring Arabian Sea and the Indian subcontinent, with a resolution of 5700 years. When combined with oxygen isotope stratigraphy, it is evident that the climate in marine isotope stages (MIS) 2, 4, and 6 is cold and dry with weakening summer wind and stronger winter winds, while the climate in MIS 1, 3, and 5 is warm and humid (Prabhu et al., 2004) with increased precipitation brought by an enhanced summer monsoon. The remaining drilling cores in the Arabian Sea are almost not more than twenty thousand years in age. Pollen deposition research of these cores shows that there were major changes in monsoon intensity occurred during the last glacial-interglacial cycles (Bentaleb et al., 1997). Pollen results of the drilling core SO90-56KA from the Makran coastal area in the Arabian Sea indicated that the end of the Holocene wet period occurred between 4700 and 4200 BP, correlating with the weakening of the Indian monsoon flux (Ivory and Lézine, 2009).

Previous studies on the Indian monsoon were mostly based on the presence of foraminifera that reflect upwelling, which in turn indirectly reflects the Indian paleo-monsoon. Conversely, pollen in deep-sea sediments can provide information on vegetation along the coast; applying direct evidence of environmental change on the continent for comparison with oceanic environmental change, especially for the reconstruction of the paleo-monsoon evolutionary history. Sediment pollen of the northeastern Indian Ocean is more easily influenced by the winter monsoon due to its proximity to the Asian continent. To date, paleoenvironmental study in this area is very rare due to sampling limitations. It is especially rare to attempt paleovegetation and paleoclimate reconstruction using pollen analysis.

The northeastern Indian Ocean has been selected as the present study area (Fig. 1). These samples (core 12I712 and YDY05) were used for paleoclimate reconstruction of the northeastern Indian Ocean and to uncover the link between the northeastern Indian Ocean and the South China Sea to discuss the historical process and correlation of the India monsoon and East Asian monsoon.

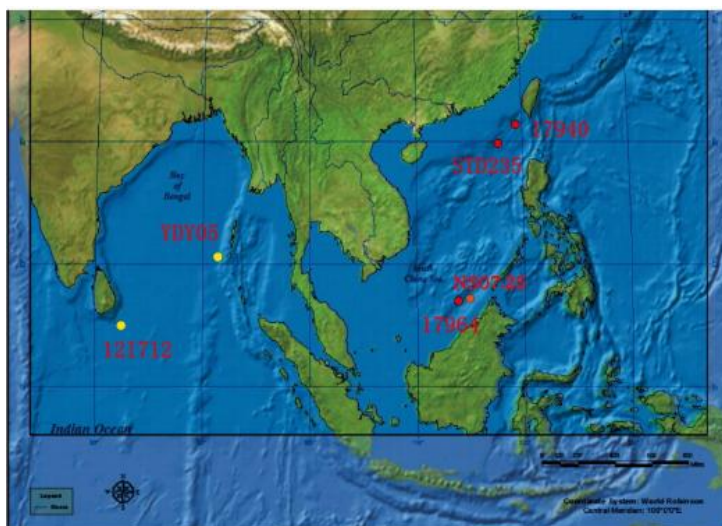


Figure1. Location of core 12I712 and YDY05 (yellow circles), core NS07-25, STD235, 17940, 17964 (red circles) (after Fang and Luo, 2015; Yu et al., 2016; Sun et al., 1999).

2. REGIONAL SETTING

2.1. Submarine Topography

The main topographical characteristics of the northeastern Indian Ocean are the countless volcanic guyots, submerged seamounts, and two subaerial islands. The northeastern Indian Ocean is separated into all types of physiographic divisions (Fig. 2) comprising the North West Shelf, Wombat Plateau, Exmouth Plateau, Cuvier Abyssal Plain, Argo Abyssal Plain, Gascoyne Abyssal Plain, and Platypus Spur (Taneja et al. 2015).

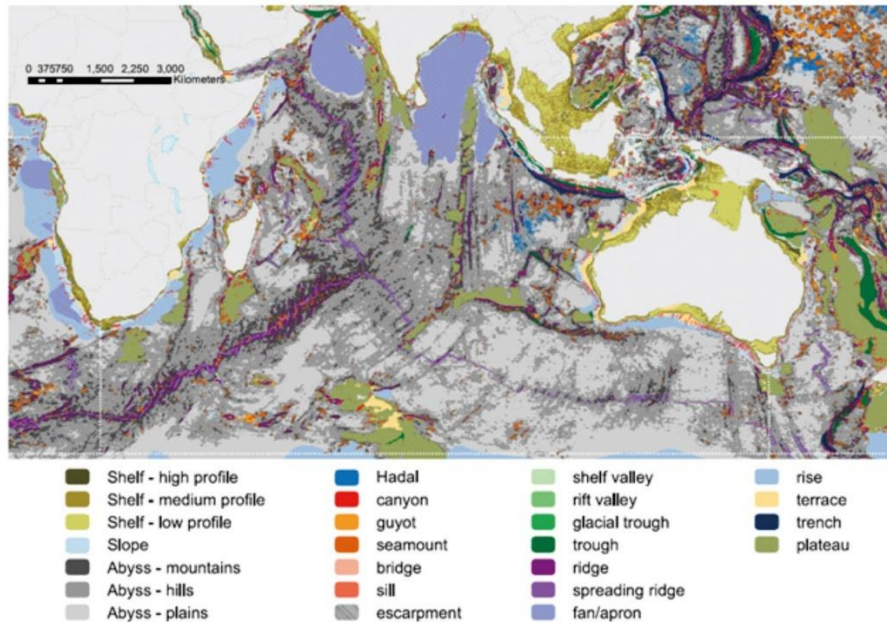


Fig. 2

Figure 2. Geomorphic features map of the Indian Ocean. Dotted white lines mark boundaries between major ocean regions. Basins are not shown (Harris et al., 2014).

The largest area of the submarine fan is located in the Indian Ocean (Fig. 2), including the two largest submarine fans in the world, the Indus and Bengal Fans (Curry et al., 2002; Covault, 2011). The largest area of slope terraces and rift valleys also occurs in the Indian Ocean (IHO, 2008). Plateaus are notable features in the Indian Ocean, covering over 8% of its area. The largest area of rift valleys also occurs in the Indian Ocean. Due to transforming faults and other factors (Macdonald, 2001), rift valley segmentation manifests as numerous smaller-sized valleys in the Indian and Pacific Oceans. The largest mean seamount size occurs in the Indian Ocean (890 km²). Terraces characterize over 21%, and they are most common on the continental slopes of the Indian Ocean. Rift valleys have the greatest area in the Indian Ocean, covering 165,220 km². Escarpments characterize 18.7% of the submarine canyons in the world and cover 17.5% of the canyons in the Indian Ocean (Harris et al., 2014).

2.2. Atmospheric Circulation and Climate

The oceanography of the Indian Ocean is characterized by tropical ocean and monsoons. The climate can be divided into four climate zones. The northeastern part of the Indian Ocean has a monsoon climate. In the summer (May to October), a strong southwest monsoon flows from the Indian Ocean to the Asian continent, carrying pollen and spores from the far African continent to the northeastern part of the Indian Ocean. In the winter (October to April), a north and northeast monsoon flows from the Asian continent to the Indian Ocean, carrying abundant tropical and subtropical pollen and spores from the Southeast and South Asian continent to the northeastern Indian Ocean (Fig. 3).

The basin-wide surface wind field is dominated by an alternation between the winter (Fig. 3a) and summer monsoons (Fig. 3c) (Hastenrath, 2007). In winter the flow from the north recurves near the equator to meet the South Indian Ocean trade winds, whereas in summer the southern trade winds recurve near the equator to flow into South Asia. During the short transition between monsoons (Figs. 3b and 3d), there are strong westerlies in the equatorial zone of the Indian Ocean. (Hastenrath, 2007).

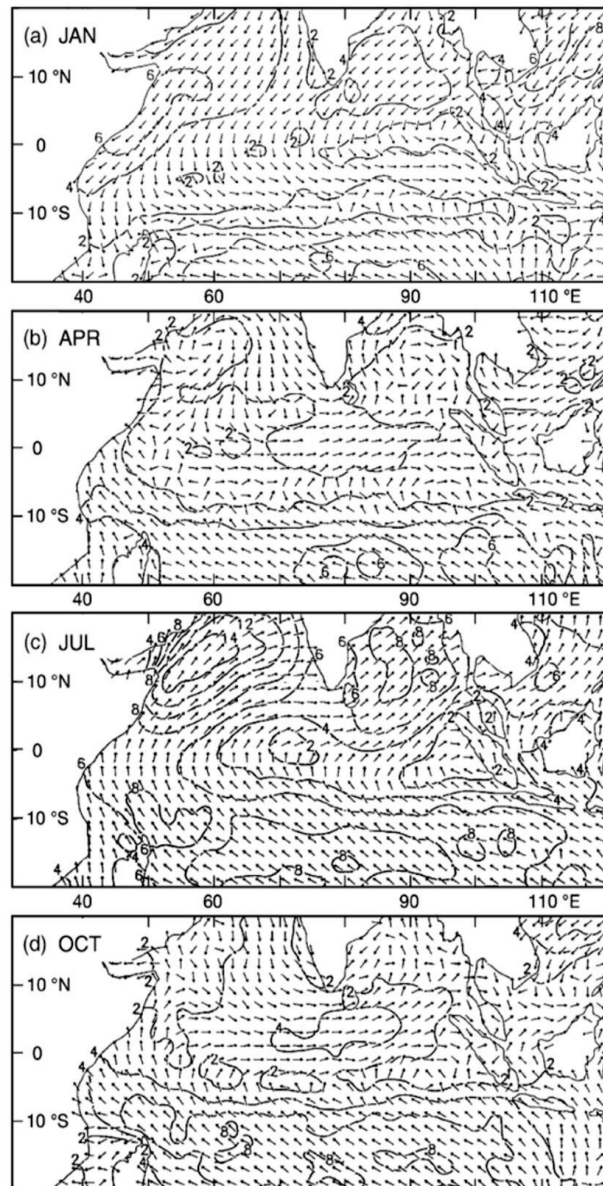


Fig. 3

Figure 3. Surface wind field over the Indian Ocean with isotach spacing of 2ms^{-1} : (a) January, (b) April, (c) July, and (d) October.) (Hastenrath et al., 2007).

2.3. Oceanic Circulation

There is a complex system of surface currents in the eastern Indian Ocean (Fig. 4) that moves according to the monsoon and exhibits an obvious seasonality (e.g., Wijffels et al., 1996, 2002; Gordon, 2005). From December to March (NW monsoon), the South Java Current (SJC), originating in the Equatorial Counter Current (ECC), flows to the southeast to meet the Leeuwin Current (LC) (e.g., Tomczak and Godfrey, 1994). There is a high volume of runoff from Sumatra and Java because there are high precipitation rates during this season. There is a buildup of a low salinity “tongue” in the SJC because of the advection of fresher water from the Java Sea through the Sunda Strait (e.g., Wijffels et al., 1996). The establishment of an active upwelling system off Java and southwest Sumatra is led by the prevailing wind direction during the SE monsoon (July–October), and the upwelling is characterized by lower sea surface temperature (SST) and higher sea surface salt (e.g., Tomczak and Godfrey, 1994). It is rather weak due to the existence of a “barrier layer” (Sprintall and Tomczak, 1992; Du et al., 2005; Qu et al., 2005; Wijffels et al., 1996). The SJC flows northwest between July and October in contrast to the boreal winter, contributing to the South Equatorial Current (SEC) instead of the LC (e.g., Quadfasel and Cresswell, 1992). The SJC reverses every three months and is characterized by a high directional variability (e.g., Wijffels et al., 1996; Hessler et al., 2013).

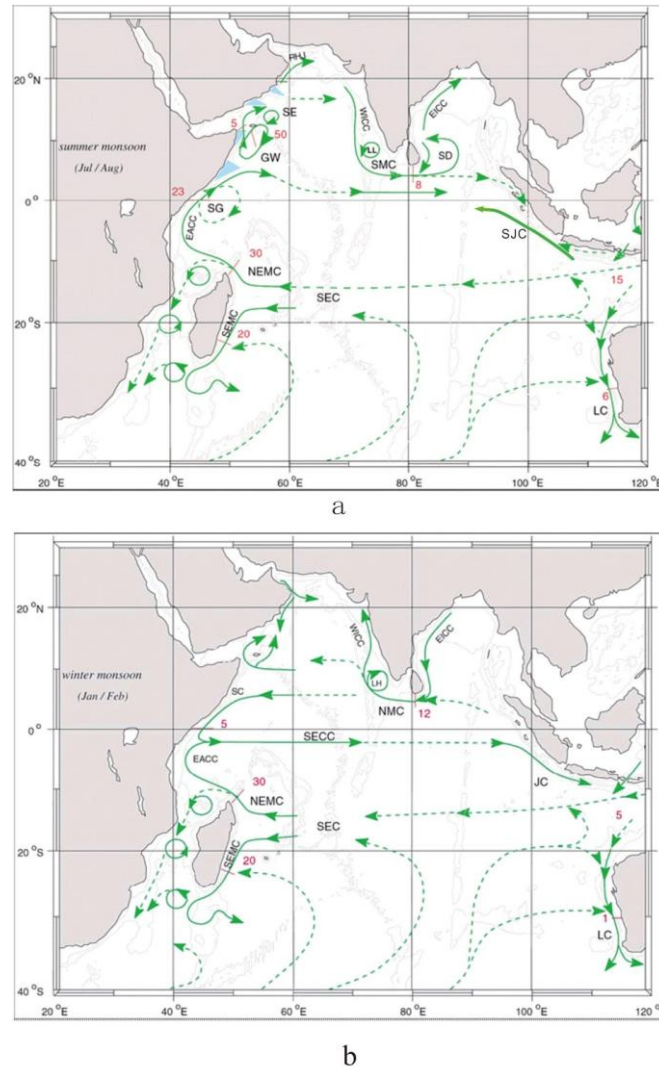


Fig. 4

Figure4a. A schematic representation of identified current branches during the Southwest Monsoon, including some choke point transport numbers ($Sv106 m^3 s^{-1}$). Current branches indicated (see also Fig. 4b) include the South Equatorial Current (SEC), South Equatorial Countercurrent (SECC), Northeast and Southeast Madagascar Currents (NEMC and SEMC), East African Coast Current (EACC), Somali Current (SC), Southern Gyre (SG), Great Whirl (GW) and associated upwelling wedges, Socotra Eddy (SE), Ras al Hadd Jet (RHJ) and upwelling wedges off Oman, West Indian Coast Current (WICC), Laccadive High and Low (LH and LL), East Indian Coast Current (EICC), Southwest and Northeast Monsoon Current (SMC and NMC), South Java Current (JC), and Leeuwin Current (LC) (e.g., Wijffels et al., 1996, 2002; Gordon, 2005; Tomczak and Godfrey, 1994; Quadfasel and Cresswell, 1992; Hessler et al., 2013);

Figure4b. As in Fig. 4a, but for the Northeast Monsoon (Schott et al., 2001). For later reference, Figs. 4a and 4b schematically illustrate the prominent surface currents during both monsoon seasons, as observed from ship-drift climatologies (Cutler & Swallow, 1984) and from drifters (Molinari et al., 1990; Shenoi et al., 1999); Schott et al., 2001).

2.4. Vegetation

2.4.1 Vegetation of Southeast Asia

1) Tropical rain forests and mountain rain forests

Tropical rain forests in Southeast Asia are mainly distributed in lowlands near the equator (normally below 600 m to 1,000 m), also known as the equatorial rain forest. Most rain forests are located in the Kalimantan Islands, Sumatra, Sulawesi, Irian Jaya, and the islands of the Malay Peninsula. They are only partially developed on the mainland, mainly distributed in the south of Vietnam, Cambodia, Thailand, and Myanmar. Lianas, or vines, are particularly lush in the rainforest of Southeast Asia. There are nine genera in the palm family. Of these, the *Calamus* genus is most widely distributed, with 72

known species of *Calamus* in Peninsular Malaysia. Of the rain forest trees, Dipterocarpaceae is the characteristic family, known as the "king of the rainforest." More than 50% of the tall trees of the upper rain forest is of the Dipterocarpaceae family (Fig.5) (Yan, 1984).

In tropical rainforest regions, low land dipterocarp forests occur at an altitude of less than 350m in Peninsular Malaysia, while hilly dipterocarp forests occur at an altitude of 350 to 850 m. Finally, upper dipterocarp forests occur at an altitude of 850 to 1,000 m. This change in altitude also marks the transition of a staggered community between lowland rain forest and mountain rain forest. Mountain rain forest typically occurs at an altitude of 1,000 to 2,500m, and the subalpine forest begins above 2,500 m (Fig.5) (Yan, 1984).

2) Tropical monsoon forest and mountain monsoon forest

In Southeast Asia, the equatorial rainforest transitions into seasonal forest on both the northern and southern hemispheres. Monsoon forests are widely distributed on Indochina north of the equator, as well as on some islands south of the equator, such as East Java and the Lesser Sunda Islands. *Tectona grandis* (Verbenaceae family) is the representative species in various types of monsoon forests in Southeast Asia, widely distributed in Myanmar, Indochina, middle and southern Vietnam, northeastern Thailand, Laos, and the Indonesian islands. Dipterocarpaceae is the main species of monsoon forest. Bamboo (Poaceae family) is lush in the seasonal rain forest; there are many bamboo species in Southeast Asia, including *Bambusa*, *Gigantochloa*, *Dendrocalamus*, etc.

Mountain monsoon forest is mainly distributed at an altitude of 1,000-2,600 meters. Pine trees are often dominant in the composition of monsoon mountain forest; this trend is more obvious with increasing altitude. *Pinus merkusii*, *Pinus kesiya*, and *Pinus insularis* are dominant pines. *Pinus merkussi* is mainly widely distributed in Myanmar, Thailand, Vietnam, Laos, Cambodia, the Philippines, and Indonesia. *Pinus insularis* is less wide spread, mainly distributed in Thailand, Vietnam, and the Philippines. *Pinus merkussi* often grows among Dipterocarpaceae species, while *Pinus insularis* often grows among *Quercus* or *Castanea* (Fig.5) (Yan, 1984).

3) Mangrove forest

Both sides of the equator of Southeast Asia hold important distributions of eastern mangrove forests. On the mainland, mangrove forests are mainly distributed on the coast of the Irrawaddy River Delta in Burma, the coastal zone of the Mekong Delta in Vietnam, and the west bank of the Malay Peninsula in Thailand. On the archipelagos, mangrove forests are mainly distributed in Kalimantan, Sumatra, Java, Sulawesi, Irian Jaya of Indonesia, and the Mindanao, Visayas, and Palawan Islands of Philippines, and along the coast of Strait of Malacca in Malaysia (Fig.5) (Yan, 1984).

There are many varieties in mangroves, about 50 to 90 species in Southeast Asia. Mangrove formations mainly consist of Rhizophoraceae, Verbenaceae, Sonneratiaceae and other families. They are distributed seaward side on ecology series. The main genera of the water coconuts include *Nipa*, *Xylocarpus*, *Heritiera*, and *Barringtonia* (Yan, 1984).

2.4.2 Vegetation in South Asia

1) Vegetation of India

India has forests, scrub/shrub lands, and grasslands of natural and semi-natural systems (Roy et al., 2015).

Tropical evergreen forests are mainly distributed in the northeast region, the Western Ghats, and the Andaman and Nicobar Islands, whereas tropical semi-evergreen forests are distributed as a transition zone between moist deciduous forests and evergreen forests. Tropical moist deciduous forests occur in strips along the eastern side of the Western Ghats, along the foothills of the Himalayas, and on the northwestern hills and the Chota Nagpur Plateau. Tropical dry deciduous forests are distributed on both sides of the Tropic of Cancer, predominantly comprising teak (*Tectona grandis*) and sal (*Shorea robusta*). The tropical thorn forests occurring in western India generally belong to thorny leguminous species. Subtropical forests comprising both dry evergreen forests and broad-leaved hill forests could be distributed in both the eastern and western Himalayas. Temperate broad-leaved forests are distributed in the eastern Himalayas between 1500 m and 3000 m elevation and the Nilgiris, the upper reaches of the Western Ghats. Temperate mixed forests include both coniferous and broad-leaved species and are

distributed in the eastern and western Himalayas (Fig. 5). Subalpine forests extend up to the tree line throughout the Himalayas and are replaced by alpine meadows, which are dry and moist. Subalpine forests are dominated by *Abeis*, *Picea*, *Betula*, and *Rhododendron* genera. Mangroves are mainly distributed in the river deltas along the coasts, such as the Sunderbans. Scrub/shrub areas and small saplings and trees are distributed in northern India, areas of southern India and the central highlands. Grasslands are both primary and secondary formations occurring in the plains, in abandoned shifting cultivation lands, along the slopes in the Himalayas and along the coasts of western India (Roy et al., 2015) (Fig. 5).

Mangroves are found along the western and eastern Indian coasts at river estuaries. There are five dominant genera (*Avicennia*, *Lumnizera*, *Phoenix*, *Rhizophora*, and *Xylocarpus*) in mangrove formations, whereas others are delineated under the broad ‘mangrove’ class (Roy et al., 2015).

2) *Vegetation in Sri Lanka*

Vegetation on Sri Lanka consists of tropical rainforest in the southwest lowlands, tropical mountain rain forest at an altitude of 1000–1800 m and tropical forest on higher altitudes. Natural forest accounted for 30.89% of the national land area in 1992. Most forest is arid monsoon forest, with a small area of tropical rainforest. The major vegetation type in the dry zone of Sri Lanka is a dry semi-evergreen forest, which includes the dry peat ssp. *Manilkara hexandra*, *Bauhinia racemosa*, and *Grewia tiliaefolia* as the most common taxa. The most common species of forest plantation are *Tectona grandis*, followed by eucalyptus (mainly *Eucalyptus grandis*), *Pinus caribaea*, and *Swietenia mahogani*.

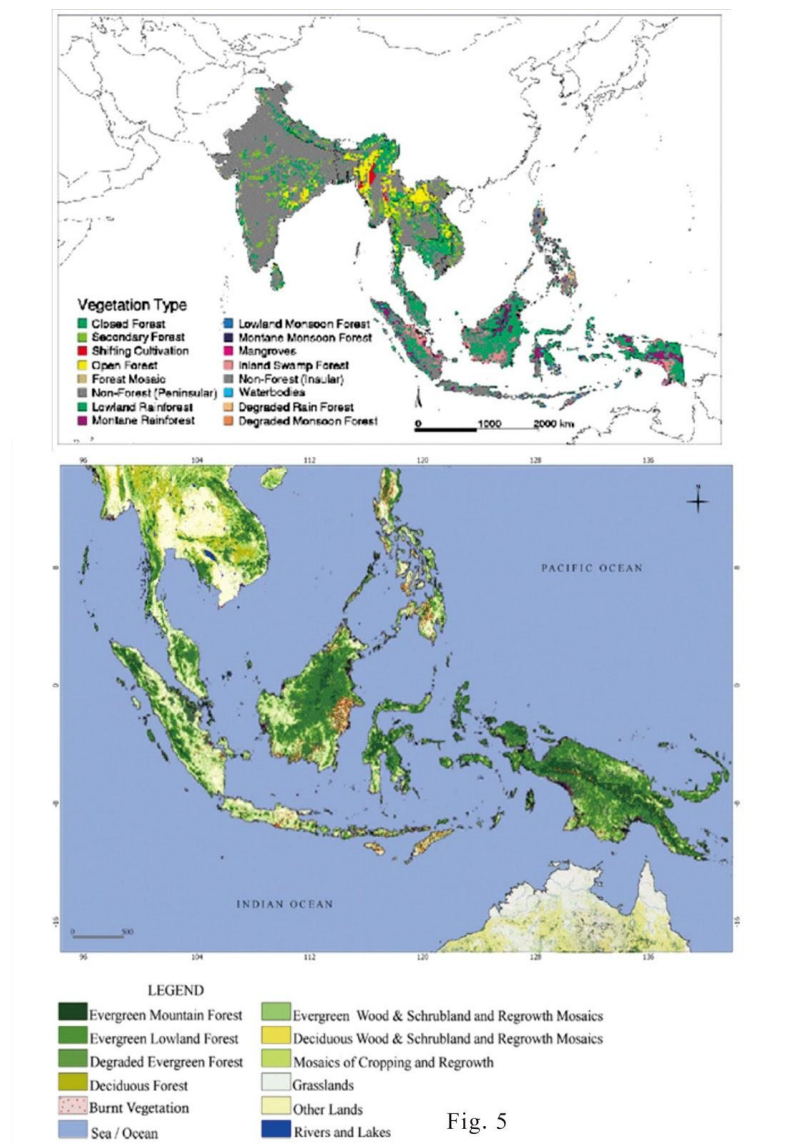


Figure5. *Vegetation type map of the northeastern Indian Ocean (Yan, 1984).*

3. MATERIALS AND METHODS

3.1. Sampling

The Gravity piston cores were collected in a No. 1 R / V Experiment boat in 2012 and 2010 by the Chinese Academy of Sciences Institute of the South China Sea. The length of core 12I712 is 265 cm, and that of YDY05 is 240 cm (Luo, et al., 2018). The samples of the 12I712 core were taken from deep basins, and those of the YDY05 core were taken from the west slope of the East Indian Range. The YDY05 core was located at a longitude of 90.32°E and latitude of 9.99°N. The core 12I712 was located at a longitudinal of 82.5°E and latitude of 4°N. The carbon isotope analyses of benthic foraminifera oxygen and AMS¹⁴C planktonic foraminifera chronostratigraphic tests were compared to establish a high-resolution chronostratigraphic sequence of nearly 45 ka BP for the 12I712 core and 43.5ka years for the YDY05 core (Fig. 6). The 12I712 core was separated and described by sampling at 1-cm intervals in the laboratory, and it was then collected at 2-cm intervals; it was analyzed by pollen from 133 samples with a 340a resolution. The YDY05 core was separated and described by sampling at 1-cm intervals in the laboratory and analyzed by pollen from 97 samples with 450 a resolution (Luo, et al., 2018).

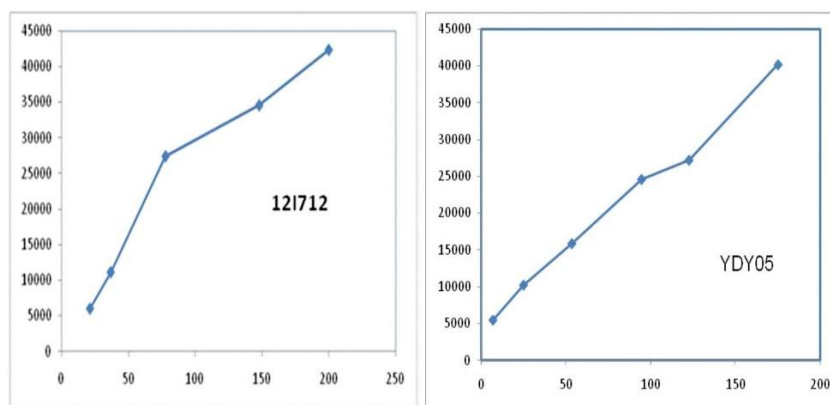


Fig.6

Figure6. Age model of core 12I712 and YDY05.

3.2. Laboratory Analysis

Samples of 4 g to 10 g were processed for pollen. We used hydrofluoric acid treatment to remove siliceous materials from the samples. Then, a heavy liquid (HBr, KI, and Zn) with a specific gravity of 2.0 ($d = 2$) was used to separate the spores and pollen by flotation. The spores and pollen were concentrated in the supernatant. Then, the supernatant was kept in other tubes, and the pollen and spore were kept in the remaining materials in the tubes after centrifugation. If there were many siliceous materials in the remaining material, then an HF acid treatment was used to remove siliceous materials. Finally, the remaining material mixed with pollen and spore was filtered through a 7- μ m nylon sieve with an ultrasonic treatment to make the slides clearer.

To calculate the pollen concentrations, we added *Lycopodium* spore tablets with a known concentration (27,637 /grains) before analyzing the samples. Maher (1971) calculated the confidence intervals that could be expressed as the significance of the pollen percentages. The presence of more than 200 pollen and spore grains per sample is the standard for a statistically significant sample. Counting pollen grains until the added *Lycopodium* spores total more than 1,000 is the standard for samples with a low pollen content.

3.3. Calculations of Pollen Percentages and Concentration

Using the total number of pollen grains from terrestrial seed plants as a base value, we calculated the percentage of each type of spore and pollen in both modern and sentimental samples. The distribution pattern of the pollen was obtained using distribution maps of the percentages of surface pollen. This distribution pattern reflects the pollen transmission route and mechanism, the distance from the shore, and the distribution patterns of pollen types. The percentage values for pollen and spores are relative. In contrast, it is absolute for the pollen concentration, and it provides a basis for comparing the amounts

of pollen or spores of a given species. Combining the two parameters, we can obtain powerful clues about the source of the pollen or spores.

The concentration was calculated in two steps. First, the relative proportions of pollen or spores were calculated, and then the number of *Lycopodium* spores was used as a reference to normalize the values:

$$R = [27637/Lycopodium \text{ number per slide}] \times [\text{pollen or spore number per slide/total weight per sample}]$$

where R is the concentration of pollen or spores. After determining the number of pollen grains or spores in each sediment sample and calculating the pollen or spore percentages and concentrations, the values were plotted on a map of the study area.

4. RESULTS

4.1. Pollen Diagram in Core 12I712 in the Northeastern Indian Ocean

According to the pollen and AMS 14C of the 12I712 core results, the pollen diagram has been divided into four distinct zones, A, B, C, and D, from bottom to top based on a Tilia and CONISS analysis, and a description of each zone is given below (Fig. 7a).

Zone A covers the period of 45~42 ka BP (265 cm- 200 cm): Qleaceae-*Alnus-Quercus-Canstanopsis-Myrtaceae*. This zone is characterized by the dominance of fern spores (45.3%), tree pollen (32.6%), and herbaceous pollen (22.1%), with an average pollen concentration of 632 grains /g.

Zone B covers the period of 42~36 ka BP (200 cm- 165 cm): Qleaceae-*Alnus-Quercus-Canstanopsis-Myrtaceae-Palmae*. This zone is characterized by the dominance of fern spores (49.37%), tree pollen (24.48%), and herbaceous pollen (26.14%) with an average pollen concentration of 964 grains /g.

Zone C covers the time span of 36~26 ka BP (165 cm-95 cm): trilete spore-monolete spore- Poaceae-Caryophyllaceae—Umbelliferae-*Pinus-Corylus*. This zone is characterized by the dominance of fern spores (53.75%), herbaceous pollen (28.10%), and tree pollen (18.15%); its pollen concentration is very low (73 grains /g).

Zone D covers the time span of 26~5 ka BP (95 cm-0 cm): trilete spore-monolete spore-Chenopodiaceae-Poaceae-Caryophyllaceae-*Pinus-Myrtaceae*. This zone is characterized by the dominance of fern spores (50%), herbaceous pollen (31.58%), and tree pollen (18.42%) ; it has the lowest pollen concentration (22 grains /g) .

4.2. Pollen Diagram in Core YDY05 in the Northeastern Indian Ocean

According to the pollen and AMS 14C results of the YDY05 core, the pollen diagram has been divided into four distinct zones, A, B, C, and D, from bottom to top based on the Tilia and Coniss analysis, and a description of each zone is given below (Fig. 7b) (Luo, et al., 2018).

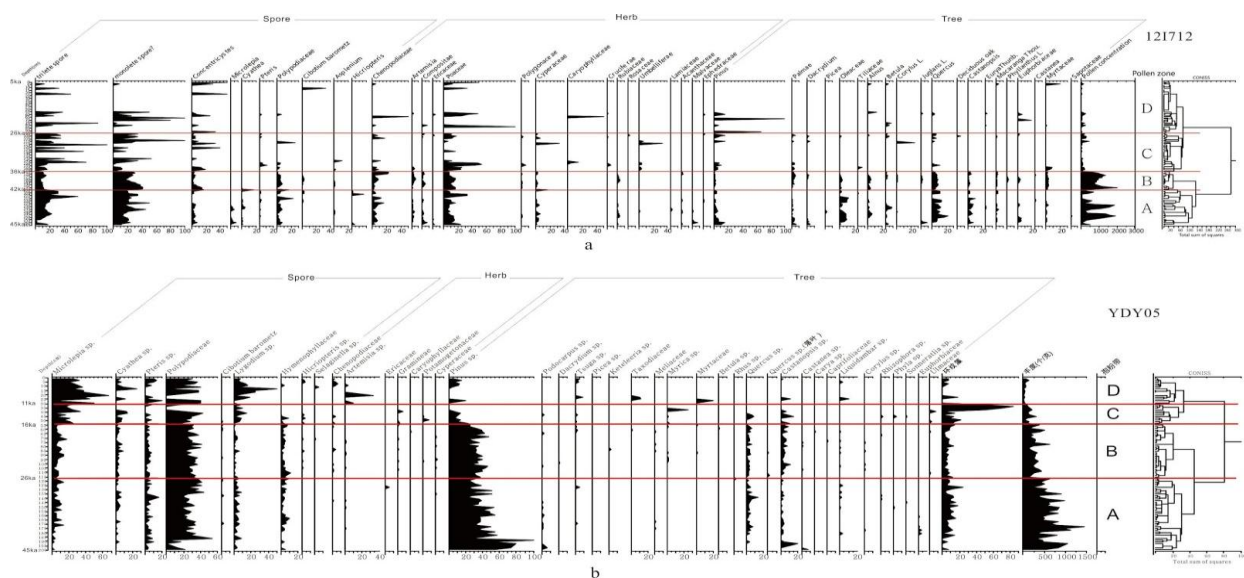


Figure 7. Pollen diagrams of core 12I712 and YDY05 (Luo, et al., 2018).

Zone A covers the time span of 45-26 ka BP (200 cm-116 cm): Polypodiaceae, *Pinus*, *Castanopsis*, evergreen *Quercus*, and *Concentricytes* are dominant.

Zone B covers the time span of 26-16 ka BP (116-54 cm): Polypodiaceae, *Pinus*, *Castanopsis*, evergreen *Quercus*, and *Concentricytes* are dominant.

Zone C covers the time of 16-11 ka BP (54-30 cm): *Microlepidia* spores, Polypodiaceae, *Myrica*, *Castanopsis*, evergreen *Quercus*, Ulmaceae, and *Concentricytes* are dominant.

Zone D covers the time span of 11 ka BP-present (30-0 cm): *Microlepidia* spores, Polypodiaceae, *Lygodium*, *Artemisia*, *Tsuga*, Taxodiaceae, Myrtaceae, and Liquidambar are dominant.

5. DISCUSSION

5.1. Pollen Sources of the Main Taxa

Tropical rain forests in Southeast Asia are mainly distributed in lowlands near the equator (normally below 600 m to 1,000 m). Most rain forests are located in the Kalimantan Islands, Sumatra, Sulawesi, Irian Jaya, and the islands of the Malay Peninsula.

Pine trees are often dominant in the composition of monsoon mountain forest; this trend is more obvious with increasing altitude. While *Pinus insularis* often grows among *Quercus* or *Castanea* in Southeast Asia. This is coherent with the results from AB, BC transects and PCA, indicating that *Pinus*, *Quercus* or *Castanopsis* are from eastern islands of the study area.

Natural and semi-natural systems in India are classified into forests, scrub/shrub lands, and grasslands on the basis of the extent of green cover (Roy et al., 2015). In Sri Lanka, most forest is arid monsoon forest, with a small area of tropical rainforest. The major vegetation type in the dry zone of Sri Lanka is dry semi-evergreen forest. Compared with larger area of closed forest in Southeast Asia, the vegetation in South Asia (India and Sri Lanka) are dryer and has more secondary forest and non-forest area (Luo et al., 2018), this might be the reason that there are more *Microlepidia* spore and herb pollen west of the boundary (90°E longitude line) based on pollen analysis results along the east-west AB and northwest-southeast BC transects (Luo et al., 2018).

5.2. Terrestrial Vegetation Changes of the 12I712 and YDY05 Cores

5.2.1 Terrestrial Vegetation Changes of the 12I712 Core

In zones A and B (45~36 ka BP) of the 12I712 core, tree pollen had a higher percentage (32.6% for A and 24.48% for B, especially the pollen of *Quercus* and *Castanopsis* (Fig. 7a); this is similar to modern sediment pollen near Sumatra Island (Luo et al., 2018), which has more tree pollen, and some of them are transported by the northwestward currents driven by the intensive summer monsoon. Combined with the high pollen concentration in A and B zones, this reflects the warm and humid climate of the resource areas, which was associated with a high sea level (Fig. 8a). Because core 12I712 is very close to India and Sri Lanka, this can indicate that the main pollen sources are India and Sri Lanka with a tropical rain forest and tropical monsoon rain forest during that period.

The percentage of pollen of the trees in zones C and D (36 ~ 5 ka BP) (18.15% for C and 18.42% for D) decreased and the percentage of pollen of the herbaceous plants increased compared with zones A and B (Fig. 7a); the pollen assemblages are similar to the pollen in the surface sediment samples of the northeastern Indian Ocean near Sri Lanka and the Indian Peninsula. The percentages of tree pollen from *Castanopsis* and evergreen *Quercus* (belonging to the subtropical zone) were lower, and the percentages of pollen from *Betula* and *Alnus* (belonging to the temperate zone) increased. The small number of pollen, low pollen concentration (73 grains/g for C and 22 grains/g for D, and increased percentage of herbaceous pollen (such as Chenopodiaceae and Poaceae) reflect the gradual transformation to a cold and dry climate with scarce vegetation and drought. At that time, the pollen source of the 12I712 core may be Sri Lanka and Eurasia (pollen source of temperate trees). Approximately 18,000 years ago, the percentages of Chenopodiaceae, Caryophyllaceae, Euphorbiaceae, *Alnus* and Pine were at their peak, reflecting the coldest and driest climate, which coincided with the time of the Last Glacial Maximum (LGM).

5.2.2 Terrestrial vegetation changes of YDY05 core

In YDY05, zones A and B cover the time span of 45-16 ka BP (200-54 cm): the dominant pollen are from trees (mainly *Pinus*, *Castanopsis* and evergreen *Quercus*) and monolet spores, with very few

herbaceous pollen; this is similar to the modern pollen diagram of Sumatra Island, with a higher percentage of cold-loving *Pinus* pollen, indicating a cool and humid climate (Fig. 7b). The climate during in 18 ka had no obvious difference compared with the upper and lower layers. Compared with the high sea level period of the Holocene, there was a shorter distance from the YDY05 core to the river estuary in the LGM, and it received a large share of pollen and spore.

Zones C and D cover the time span of 16 ka BP-present (54-0 cm): the percentage of *Microlepidia* spores increased sharply, and the dominant pollen come from a larger variety of trees (*Myrica*, *Castanopsis*, evergreen *Quercus*, Ulmaceae, *Tsuga*, Taxodiaceae, Myrtaceae, and Liquidambar) (Fig. 7b); this is similar to the modern pollen diagram of Sri Lanka Island, with more herbaceous and trilete spores (Luo et al., 2018) indicating a warm and dry climate. In the previous study, the percentage of fern in the southern South China Sea was useful as a proxy for the summer monsoon (Sun et al., 1997). In the present study, it was found that in the NS07-25 and STD235 cores from the South China Sea and the YDY05 core from the northeastern Indian Ocean, the percentage of fern spores also increased in the interglacial period with the intensive summer monsoon (Fig. 8).

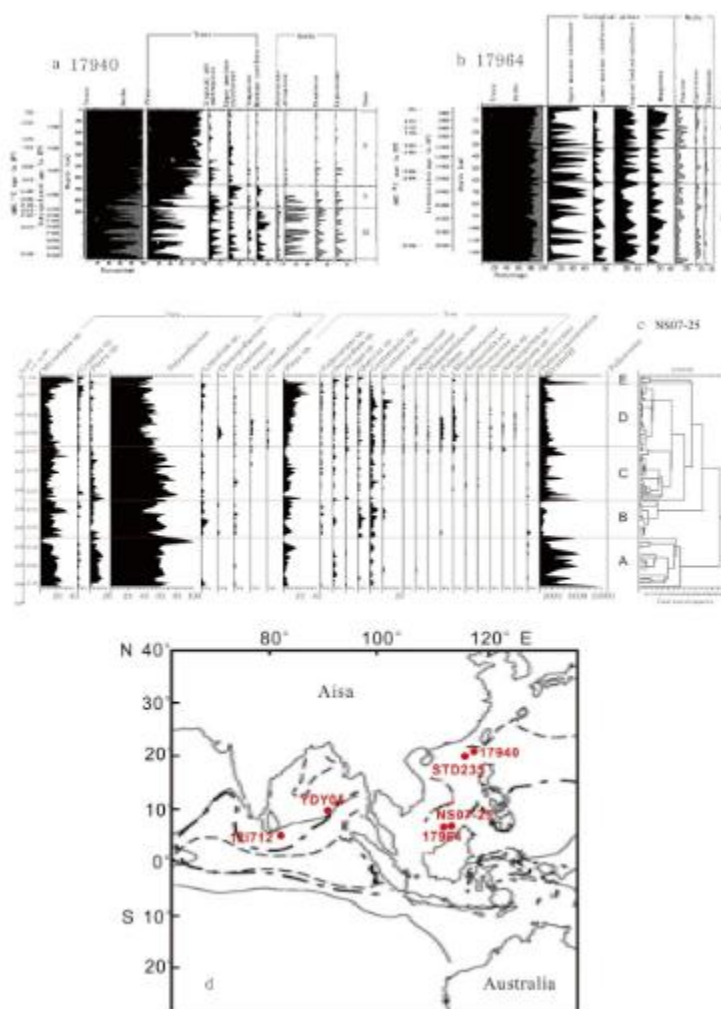


Figure 8a. Pollen diagram of core 17940 (after Sun et al., 1999); b. Pollen diagram of core 17964 (after Sun et al., 1999); c. Pollen diagram of core NS07-25 (red circles) (after Fang and Luo, 2015); d. The 28.5 C isotherm is the boundary for the warm pool (thin full lines: 28.5C isotherm on average in March for 50 years; the dotted line: the annual average of 28.5 isotherms in August; the dot dashed line: an annual average of approximately 28.5 isotherms (Yang et al., 2007), on the basis of an average of 50 years).

Based on the analysis of fossil pollen from YDY05 core in the northeast Indian Ocean, we determined that since 16ka BP, the land source of pollen may have shifted from Sumatra Island to Sri Lanka island and India, which may be related to sea level changing (Fig. 9): 16 ka BP-26 ka BP has a low sea level of -105 m to -134 m (Fig. 9c, Fig. 9d), Sumatra Island is connected with Indo Peninsula, forming Sunda

continental shelf. Since 16 ka BP, sea level has risen and remained at a high level (above -105 m) (Fig. 9a, Fig. 9b), Sunda Shelf is submerged under the sea level, Sumatra island is separated from Indo Peninsula, and vegetation is not as abundant as in 16 ka BP-26 ka BP. Therefore, the source of pollen in YDY05 core may shift from Sumatra Island to Sri Lanka Island and India.

At approximately 11 ka BP, the *Concentricytes* (Freshwater algae fossils) were predominant, indicating that the runoff of the rivers, the Brahmaputra River and the Ganga River, was the largest. This is because the YDY05 core is located in the warm pool of the eastern Indian Ocean near the Bay of Bengal.

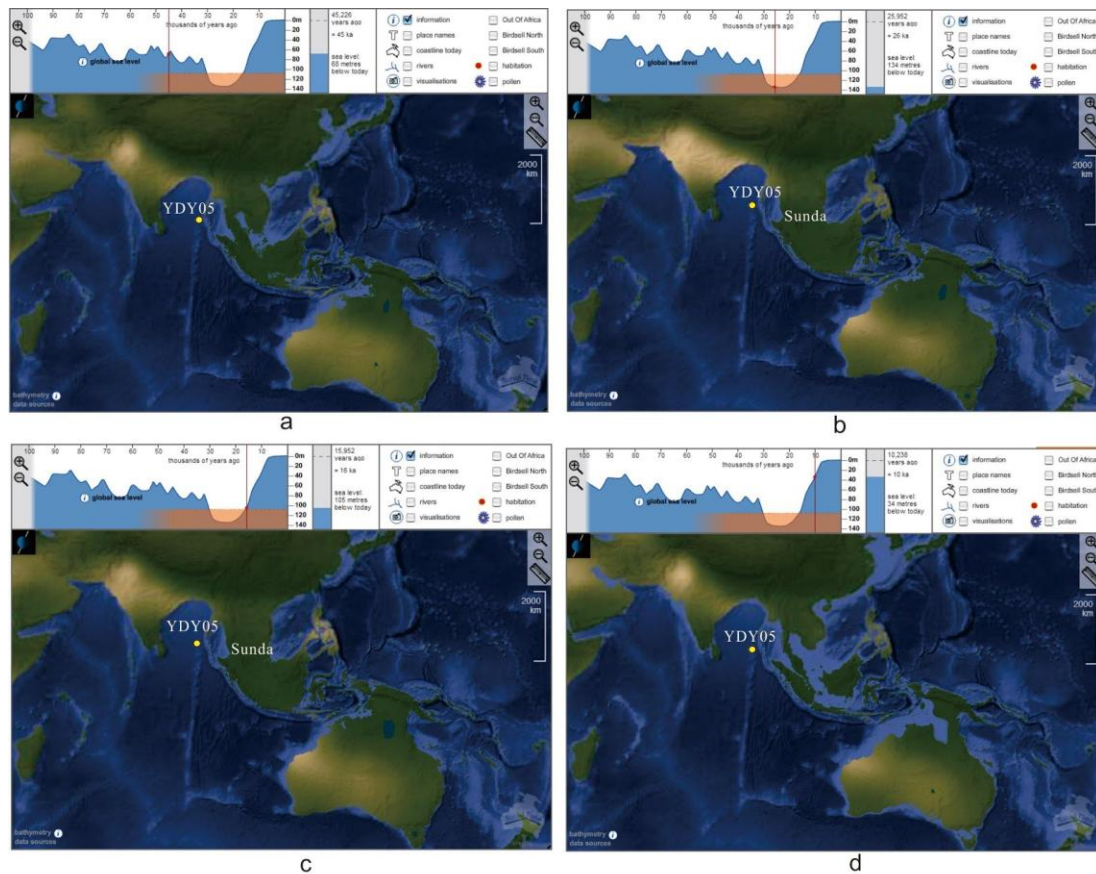


Fig. 9

Figure 9. Sea levels at 10 ka BP, 16 ka BP, 26ka BP, 45 ka BP. Retrieved from: <http://www.sahultime.monash.edu.au/explore.html>

5.2.3 Comparing the pollen of the 121712core with the YDY05 core

According to the PCA analysis of the surface pollen samples in the northeast Indian Ocean (Luo et al., 2018), one of the main factors that can affect the percentage of pollen in the study area may be the distance of the samples from the lands around the study area.

From the above analysis, we know that the YDY05 core has a different location than the 121712 core. YDY05 is located in the warm pool of the eastern Indian Ocean and near the Bay of Bengal, whereas 121712 is located in the ocean south of Sri Lanka. The two cores have different pollen sources. The pollen concentration decreased suddenly, and the herbaceous pollen increased gradually after 16 ka BP in the YDY05 core and 36 ka BP in the 121712 core, respectively, indicating that the climate gradually became dry after that time. At approximately 18 ka BP in the 121712 core, there was a coldest and driest climate in the pollen resource area.

The climate of the YDY05 core lagged 20,000 years behind the 121712 core to be dry probably because the YDY05 core was located in the warm pool of the eastern Indian Ocean before 16 ka BP. The vegetation and climate were relatively humid within the pollen resource islands close to the warm pool. Another explanation is that the warm pool of the eastern Indian Ocean was probably distributed at the location of the 121712 core before 36 ka BP, but it shrunk eastward after that time until 16 ka BP, when it completely retreated from the location of YDY05.

5.3. Comparing the Pollen of Cores in the Indian Ocean and the South China Sea

The vegetation in Sri Lanka and South Asia during the Last Glacial Maximum (LGM) based on the pollen from 12I712 and YDY05 in the northeastern Indian Ocean was different from the vegetation on the emerged continental shelves of the northern and southern South China Sea (SCS) during the Last Glacial Maximum (LGM) based on the pollen of hemipelagic sediments from the 17940 and 17964 cores (Fig. 1).

5.3.1 Warm pool as an index of climate humidity

The study of paleoclimate using the monsoon and tropical process as a basis is focused on hydrological circulation and dry and wet changes (Wang, 2009). During the LGM (including the top of the Stage 3 oxygen isotope), both the northern and southern continental shelves of the SCS were exposed. The northern continental shelf was covered by grasslands mainly of *Artemisia* based on the pollen analysis of the 17940 core. The climate should be cold and dry, but on the southern continental shelf (Sunda Land) tropical lowland rainforest prevailed and mangroves were scattered by the river mouths and along the coast based on the pollen analysis of the 17964 core. The climate of the southern continental shelf might be cooler than that of the present day, but a decrease in humidity was not observed. Significant differences of the evolution of vegetation and climate between the northern and southern continental shelf during the Last Glacial Maximum may be related to the special location of the Southern Sunda Shelf (within the warm pool of the western Pacific) (Sun et al., 1999) (Fig. 8).

According to previous studies comparing the sedimentary types and rates, strong differences in the sedimentary environment of the southern and northern South China Sea did not occur until approximately 3,000,000 years ago. That was when the modern warm pool occurred (Wang et al., 2003). During the MIS 2/3 transition period (29 ~ 25 ka BP), the western Pacific warm pool may have moved westward. From 22.5 to 16.5 ka BP, the warm pool may have moved westward to the south of the South China Sea (Chen et al., 2005).

The proportions of herbaceous pollen in the YDY05 and 17964 cores did not increase in 18 ka BP, indicating that the climate was not dry at that time. The 17964 core was probably located in the western Pacific warm pool, and the YDY05 core was within the warm pool of the eastern Indian Ocean. Meanwhile, the dominant pollen of 12I712 and 17940 were herbaceous plants during 18 ka BP, the last glacial period, reflecting the characteristics of a cold and dry climate. This indicates that the temperature of the northeastern coast of the Indian Ocean and the northern coast of SCS had decreased during the Last Glacial Maximum and that the humidity was also significantly decreased, relating to their location outside of the warm pool of the western Pacific - eastern Indian Ocean (Fig. 8). Warm pools can be taken as an index of climate humidity in the present study, and the climate change during glacial cycles of the southern SCS and the Indian Ocean are related to the low altitude tropical process. This indicates that monsoons in the southern SCS (mainly referring to summer monsoons) are closely related to solar radiation, coinciding with the view of Zhisheng et al. (1990) that the main dynamic mechanism of the East Asia monsoon is solar radiation.

Vegetation during the LGM on the exposed continental shelf of north SCS was predominantly grassland and/or wetland with sparse subtropical trees in the 12I712, 17940 and STD 235 cores but not in the YDY05 and 17964 cores. The widespread grass communities on the coastal-shelf of the SCS reflect the lower precipitation during the LGM in the 12I712, 17940 and STD 235 cores. Similar changes were also recorded on the continental shelf of the East China Sea, suggesting a synchronous decline in the effectiveness of the Asian summer monsoon (Zheng et al., 2013, 2011). During the LGM, more tree pollen was found in the YDY05 and 17964 cores (Fig. 8).

5.3.2 Pinus as an index of sea level change

In the STD 235 core of the northern continental shelf in the SCS, during glacial periods, a decrease in sea level reduced the distance to the shore, and fluvially derived pollen from more coastal vegetation can better reach the deep sea; hence, the percentage of *Pinus* decreased. As sea level rises in the deglacial, the distance to the coast increases, increasing the relative amount of *Pinus* pollen in the marine sediments due to the strong transporting capacity for pine pollen and decreasing the relative amount of other pollen and spores (Yu et al., 2016). Similar results have been found in the 17940 core (Sun et al., 1999) in the northern SCS and core NS07-25 in the southern SCS (Fang and Luo, 2016), the Gulf of

Lion (Western Mediterranean Sea) (Beaudouin et al., 2007) and the Okinawa Trough (Zheng et al., 2011) on sites near the continent shelf (Fig. 8).

However, in 12I712 and YDY05 in the northeast Indian Ocean, the situation is the reverse. *Pinus* pollen increased from the deglacial to glacial periods in YDY05 and in 12I712 (Fig. 8), these differences of *Pinus* pollen percentage may be due to the difference in the topography of the cores. The 12I712 and YDY05 cores are located in the deep-sea basin of the Indian Ocean, where the continental shelves of the nearby island or land are very narrow. A decline in sea-level in the LGM did not expand the exposed lands around the northeastern Indian Ocean, and the distance from the core to the shore had no obvious change. Thus, the pollen of the coastal vegetation did not reach the deep sea and the percentage of *Pinus* was still high in the pollen component.

6. CONCLUSION

(1) In zones A and B (45~36 ka BP) of the 12I712 core, tree pollen had a higher percentage. Combined with the high pollen concentration in A and B zones, this reflects the warm and humid climate of the resource areas, which was associated with a high sea level. The percentage of pollen of the trees in zones C and D (36 ~ 5 ka BP) decreased and the percentage of pollen of the herbaceous plants increased. The percentages of tree pollen from *Castanopsis* and evergreen *Quercus* were lower, and the percentages of pollen from *Betula* and *Alnus* increased, reflecting the gradual transformation to a cold and dry climate with scarce vegetation and drought.

(2) Differences in the evolution of vegetation and climate between the northern and southern continental shelf in the SCS during the LGM occurred because the Southern Sunda Shelf is located in the warm pool of the western Pacific. Similar results have been found in the northeastern Indian Ocean. During the LGM, more tree pollen was found in the YDY05, 17964 and STD 235 cores, indicating that the climate of the pollen source was still humid and that the cores were located in the warm pool. During the LGM, more herbaceous pollen was found in the 12I712 and 17940 cores, indicating that the climate of the pollen source was dry and that the cores were located outside of the warm pool.

(3) Comparing the pollen of the cores in the Indian Ocean with those from the South China Sea, *Pinus* was found to be an index of sea level change: during glacial periods, a decrease in sea level reduced the percentage of *Pinus* only in the cores near the continent shelves, such as in the northern and southern SCS. However, the percentage of *Pinus* pollen increased in the glacial period in the northeastern Indian Ocean because the cores were almost in the deep sea and the sea level change did not affect the distances of pollen sources.

ACKNOWLEDGMENTS

This work was funded by the National Natural Science Foundation of China (grants NSFC 41876062, 41676047, 91228207).

REFERENCES

- [1] Zhisheng, A., Tunghseng, L., Yanchou, L., Porter, S.C., Kukla, G.H.W.X., Xihao, W. and Yingming, H., 1990. The long-term paleomonsoon variation recorded by the loess-paleosol sequence in central China. *Quaternary International*, 7, pp.91-95.
- [2] Beaudouin, C., Suc, J. P., Escarguel, G., Arnaud, M., & Charmasson, S. (2007). The significance of pollen signal in present-day marine terrigenous sediments: the example of the Gulf of Lions (western Mediterranean Sea). *Geobios*, 40(2), 159-172.
- [3] Bentaleb, I., Caratini, C., Fontugne, M., Morzadec-Kerfourn, M. T., Pascal, J. P., & Tissot, C. (1997). Monsoon regime variations during the late Holocene in the southwestern India. In *Third Millennium BC Climate Change and Old World Collapse* (pp. 475-488). Springer, Berlin, Heidelberg.
- [4] Chauhan, M. S., Pokharia, A. K., & Srivastava, R. K. (2015). Late Quaternary vegetation history, climatic variability and human activity in the Central Ganga Plain, deduced by pollen proxy records from Karela Jheel, India. *Quaternary International*, 371, 144-156.
- [5] Chen, M., Li, Q., Zheng, F., Tan, X., Xiang, R., & Jian, Z. (2005). Variations of the Last Glacial Warm Pool: Sea surface temperature contrasts between the open western Pacific and South China Sea. *Paleoceanography*, 20(2).
- [6] Clemens, S., Prell, W., Murray, D., Shimmield, G., & Weedon, G. (1991). Forcing mechanisms of the Indian Ocean monsoon. *Nature*, 353(6346), 720-725.

- [7] Clemens, S. C., Murray, D. W., & Prell, W. L. (1996). Nonstationary phase of the Plio-Pleistocene Asian monsoon. *Science*, 274(5289), 943-948.
- [8] Covault, J. A. (2011). Submarine fans and canyon-channel systems: a review of processes, products, and models. *Nature Education Knowledge*, 3(10), 4.
- [9] Curray, J. R., Emmel, F. J., & Moore, D. G. (2002). The Bengal Fan: morphology, geometry, stratigraphy, history and processes. *Marine and Petroleum Geology*, 19(10), 1191-1223.
- [10] Cutler, A. N., & Swallow, J. C. (1984). Surface currents of the Indian Ocean (to 25°S, 100°E): compiled from historical data archived by the Meteorological Office, Bracknell, UK, Rep. 187, 8pp, 36 charts, Inst. of Oceanogr. Sci., Wormley, England.
- [11] Demske, D., Tarasov, P. E., Wünnemann, B., & Riedel, F. (2009). Late glacial and Holocene vegetation, Indian monsoon and westerly circulation in the Trans-Himalaya recorded in the lacustrine pollen sequence from Tso Kar, Ladakh, NW India. *Palaeogeography, Palaeoclimatology, Palaeoecology*, 279(3-4), 172-185.
- [12] Du, Y., Qu, T., Meyers, G., Masumoto, Y., & Sasaki, H. (2005). Seasonal heat budget in the mixed layer of the southeastern tropical Indian Ocean in a high-resolution ocean general circulation model. *Journal of Geophysical Research: Oceans*, 110(C4).
- [13] Fang, X.D., Luo, C.X., (2016). Paleoclimate reconstruction since 40,000 in NS07-25 core in Southern South China Sea based on pollen data, University of Guangzhou, Undergraduate paper (*unpublished*).
- [14] Gordon, A.L. (2005). From the Guest Editor: Oceanography of the Indonesian seas. *Oceanography*, 18(4):13.
- [15] Gupta, S. M. (2003). Orbital frequencies in radiolarian assemblages of the central Indian Ocean: implications on the Indian summer monsoon. *Palaeogeography, Palaeoclimatology, Palaeoecology*, 197(1-2), 97-112.
- [16] Harris, P. T., Macmillan-Lawler, M., Rupp, J., & Baker, E. K. (2014). Geomorphology of the oceans. *Marine Geology*, 352, 4-24.
- [17] IHO., (2008). Standardization of Undersea Feature Names: Guidelines Proposal Form Terminology, 4th ed. International Hydrographic Organization and Intergovernmental Oceanographic Commission, Monaco.
- [18] Hastenrath, S. (2007). Circulation mechanisms of climate anomalies in East Africa and the equatorial Indian Ocean. *Dynamics of Atmospheres and Oceans*, 43(1-2), 25-35.
- [19] Hessler, I., Young, M., Holzwarth, U., Mohtadi, M., Lückge, A., & Behling, H. (2013). Imprint of eastern Indian Ocean surface oceanography on modern organic-walled dinoflagellate cyst assemblages. *Marine Micropaleontology*, 101, 89-105.
- [20] Ivory, S. J., & Lézine, A. M. (2009). Climate and environmental change at the end of the Holocene Humid Period: A pollen record off Pakistan. *Comptes Rendus Geoscience*, 341(8-9), 760-769.
- [21] Brock, J. C., McClain, C. R., Anderson, D. M., Prell, W. L., & Hay, W. W. (1992). Southwest monsoon circulation and environments of recent planktonic foraminifera in the northwestern Arabian Sea. *Paleoceanography*, 7(6), 799-813.
- [22] Leipe, C., Demske, D., Tarasov, P. E., & Members, H. P. (2014). A Holocene pollen record from the northwestern Himalayan lake Tso Moriri: implications for palaeoclimatic and archaeological research. *Quaternary International*, 348, 93-112.
- [23] Leipe, C., Demske, D., Tarasov, P. E., Wünnemann, B., Riedel, F., & Members, H. P. (2014). Potential of pollen and non-pollen palynomorph records from Tso Moriri (Trans-Himalaya, NW India) for reconstructing Holocene limnology and human–environmental interactions. *Quaternary International*, 348, 113-129.
- [24] Liang, F., Brook, G. A., Kotlia, B. S., Railsback, L. B., Hardt, B., Cheng, H., ... & Kandasamy, S. (2015). Panigarh cave stalagmite evidence of climate change in the Indian Central Himalaya since AD 1256: Monsoon breaks and winter southern jet depressions. *Quaternary Science Reviews*, 124, 145-161.
- [25] Lin, G., Luo, C.X., (2016). Characteristics of pollen and the environmental significance of the northern part of Kalimantan island near south of the South China Sea, University of Guangzhou, Undergraduate paper (*unpublished*).
- [26] Luo, C., Chen, C., Xiang, R., Jiang, W., Liu, J., Lu, J., ... & Yang, M. (2018). Study of modern pollen distribution in the northeastern Indian Ocean and their application to paleoenvironment reconstruction. *Review of Palaeobotany and Palynology*, 256, 50-62.
- [27] Ridge, P. M. O. (2001). Mid-ocean ridge tectonics, volcanism and geomorphology. *Geology*, 26(455), 458.
- [28] Maher, L. J. (1972). Absolute pollen diagram of Redrock Lake, Boulder County, Colorado. *Quaternary Research*, 2(4), 531-553.
- [29] Murgese, D. S., & De Deckker, P. (2005). The distribution of deep-sea benthic foraminifera in core tops from the eastern Indian Ocean. *Marine Micropaleontology*, 56(1-2), 25-49.

- [30] Marret, F., & de Vernal, A. (1997). Dinoflagellate cyst distribution in surface sediments of the southern Indian Ocean. *Marine Micropaleontology*, 29(3-4), 367-392.
- [31] Molinari, R. L., Olson, D., & Reverdin, G. (1990). Surface current distributions in the tropical Indian Ocean derived from compilations of surface buoy trajectories. *Journal of Geophysical Research: Oceans*, 95(C5), 7217-7238.
- [32] Prabhu, C. N., Shankar, R., Anupama, K., Taieb, M., Bonnefille, R., Vidal, L., & Prasad, S. (2004). A 200-ka pollen and oxygen-isotopic record from two sediment cores from the eastern Arabian Sea. *Palaeogeography, Palaeoclimatology, Palaeoecology*, 214(4), 309-321.
- [33] Prell, W. L. (1984). Monsoonal climate of the Arabian Sea during the late Quaternary: a response to changing solar radiation. In *Milankovitch and climate; understanding the response to astronomical forcing: NATO advanced research. Workshop* (pp. 349-366).
- [34] Prell, W. L. (1984). Variation of monsoonal upwelling: a response to changing solar radiation. *Climate processes and climate sensitivity*, 29, 48-57.
- [35] Premathilake, R., & Seneviratne, S. (2015). Cultural implication based on pollen from the ancient mortuary complex in Sri Lanka. *Journal of Archaeological Science*, 53, 559-569.
- [36] Rawat, S., Gupta, A. K., Sangode, S. J., Srivastava, P., & Nainwal, H. C. (2015). Late Pleistocene–Holocene vegetation and Indian summer monsoon record from the Lahaul, northwest Himalaya, India. *Quaternary Science Reviews*, 114, 167-181.
- [37] Riedel, N., Stebich, M., Anoop, A., Basavaiah, N., Menzel, P., Prasad, S., ... & Wiesner, M. (2015). Modern pollen vegetation relationships in a dry deciduous monsoon forest: A case study from Lonar Crater Lake, central India. *Quaternary International*, 371, 268-279.
- [38] Roy, P. S., Behera, M. D., Murthy, M. S. R., Roy, A., Singh, S., Kushwaha, S. P. S., ... & Gupta, S. (2015). New vegetation type map of India prepared using satellite remote sensing: Comparison with global vegetation maps and utilities. *International Journal of Applied Earth Observation and Geoinformation*, 39, 142-159.
- [39] van der Kaars, S., & De Deckker, P. (2003). Pollen distribution in marine surface sediments offshore Western Australia. *Review of Palaeobotany and Palynology*, 124(1-2), 113-129.
- [40] Schott, F. A., & McCreary Jr, J. P. (2001). The monsoon circulation of the Indian Ocean. *Progress in Oceanography*, 51(1), 1-123.
- [41] Sheno, S. S. C., Saji, P. K., & Almeida, A. M. (1999). Near-surface circulation and kinetic energy in the tropical Indian Ocean derived from Lagrangian drifters. *Journal of Marine Research*, 57(6), 885-907.
- [42] Sun, X.J., Chen, X. D., Luo, Y. L., Li, X. (1999). An Insight into Paleovegetation on the Emerged Shelf at the Last Glaciation: Pollen Data of the South China Sea. *Acta Botanica Sinica*, 41(9), 1016-1023.
- [43] Taneja, R., O'Neill, C., Lackie, M., Rushmer, T., Schmidt, P., & Jourdan, F. (2015). 40Ar/39Ar geochronology and the paleoposition of Christmas Island (Australia), Northeast Indian Ocean. *Gondwana Research*, 28(1), 391-406.
- [44] Tomczak, M., & Godfrey, J. S. (2013). *Regional oceanography: an introduction*. Elsevier.
- [45] Qu, T., Du, Y., Meyers, G., Ishida, A., & Wang, D. (2005). Connecting the tropical Pacific with Indian Ocean through South China Sea. *Geophysical Research Letters*, 32(24).
- [46] Quadfasel, D., & Cresswell, G. R. (1992). A note on the seasonal variability of the South Java Current. *Journal of Geophysical Research: Oceans*, 97(C3), 3685-3688.
- [47] Wang, P., Jian, Z., Zhao, Q., Li, Q., Wang, R., Liu, Z., ... & Fang, D. (2003). Evolution of the South China Sea and monsoon history revealed in deep-sea records. *Chinese Science Bulletin*, 48(23), 2549-2561.
- [48] Wang, P. (2009). Global monsoon in a geological perspective. *Chinese Science Bulletin*, 54(7), 1113-1136.
- [49] Wijffels, S. E., Toole, J. M., Bryden, H. L., Fine, R. A., Jenkins, W. J., & Bullister, J. L. (1996). The water masses and circulation at 10°N in the Pacific. *Deep Sea Research Part I: Oceanographic Research Papers*, 43(4), 501-544.
- [50] Wijffels, S., Sprintall, J., Fieux, M., & Bray, N. (2002). The JADE and WOCE I10/IR6 through flow sections in the southeast Indian Ocean. Part 1: Water mass distribution and variability. *Deep Sea Research Part II: Topical Studies in Oceanography*, 49(7-8), 1341-1362.
- [51] Yan, C.C. (1984). Types and distribution patterns of vegetation in southeastern Asia. *Chinese Journal of Ecology*, 5.
- [52] Yang, Y., Huang, F., & Wang, D. (2007). The variation of the Indo-Pacific Warm pool. *Oceanologia et Limnologia Sinica*, 38(4), 296.

- [53] Yu, S., Zheng, Z., Chen, F., Jing, X., Kershaw, P., Moss, P., ... & Huang, K. (2017). A last glacial and deglacial pollen record from the northern South China Sea: New insight into coastal-shelf paleoenvironment. *Quaternary Science Reviews*, 157, 114-128.
- [54] Zheng, Z., Yang, S., Deng, Y., Huang, K., Wei, J., Berne, S., & Suc, J. P. (2011). Pollen record of the past 60 ka BP in the Middle Okinawa Trough: Terrestrial provenance and reconstruction of the paleoenvironment. *Palaeogeography, Palaeoclimatology, Palaeoecology*, 307(1-4), 285-300.
- [55] Zheng, Z., Huang, K., Deng, Y., Cao, L., Yu, S., Suc, J. P., ... & Guichard, F. (2013). A ~ 200 ka pollen record from Okinawa Trough: Paleoenvironment reconstruction of glacial-interglacial cycles. *Science China Earth Sciences*, 56(10), 1731-1747.

Citation: Chuanxiu Luo, et al., " Sedimental Pollen Distribution in the Northeastern Indian Ocean and their Palaeo-Environmental Information", *International Journal of Research in Environmental Science (IJRES)*, vol. 6, no. 3, pp. 9-20, 2020. Available: DOI: <http://dx.doi.org/10.20431/2454-9444.0603001>

Copyright: © 2020 Authors. This is an open-access article distributed under the terms of the Creative Commons Attribution License, which permits unrestricted use, distribution, and reproduction in any medium, provided the original author and source are credited.